J Sol-Gel Sci Technol (2012) 63:258–265
DOI 10.1007/s10971-012-2696-8

ORIGINAL PAPER

# Charged silsesquioxane used as a vehicle for gold nanoparticles to perform the synthesis of catalyst xerogels

**Michael R. Nunes · Yoshitaka Gushikem · Richard Landers · Jairton Dupont · Tania M. H. Costa · Edilson V. Benvenutti**

Received: 9 November 2011 / Accepted: 17 January 2012 / Published online: 1 February 2012
© Springer Science+Business Media, LLC 2012

**Abstract** The water soluble charged silsesquioxane that contains the bridged 1,4-diazoniabicyclo[2.2.2]octane chloride group, was used as stabilizing agent and size controller in the synthesis of gold nanoparticles smaller than 15 nm in aqueous medium. The gold nanoparticle dispersion was converted in solid powder form by evaporation. This powder presented organized structure imposed by the presence of charged organic group, similar to organized structure already observed for pure silsesquioxane. The gold nanoparticles in solid powder form presented high storage stability for several months, at ambient conditions, and can be completely redispersed in water again. After redispersion, the optical properties of gold nanoparticles, observed by ultra-violet and visible spectroscopy, and their morphological characteristics, investigated by transmission electron microscopy, are preserved. The gold nanoparticle aqueous dispersion was used as a vehicle of nanoparticles in the synthesis of sol–gel silica based hybrid material. This xerogel was characterized by $N_2$ adsorption–desorption isotherms, showing 260 $m^2g^{-1}$, and it was applied in a satisfactory way as catalyst for *p*-nitrophenol reduction to *p*-aminephenol.

**Keywords** Metal nanoparticle powder · Ionic silsesquioxane · Charged silane · Gold nanoparticle storage · Gold xerogel catalyst

## 1 Introduction

Silica materials are a very suitable media to support gold nanoparticles due to its inherent characteristics as chemical inertness, mechanical rigidity, swelling resistance, thermal stability, optical transparency and others. Considering these characteristics several systems silica/gold nanoparticles have been studied in the last decade aiming numerous applications, mainly as catalysts, sensors and biosensors [1–7]. In a general way these systems are obtained by reduction in situ of gold salt solutions or starting from nanoparticle aqueous dispersions used as precursors. In these dispersions, several stabilizing agents were applied; however, their stability, storage and transport are still a subject to be improved. In general, the commercially available nanoparticles are dispersed in liquid medium, and it is very difficult to find nanoparticles in commercial products accessible in powder form. In this context, it is very important the search for new stabilizing agents for nanoparticle that allow the preparation of stable aqueous dispersions and also metal nanopowders, which can be easily storage and transported to be used as nanoparticle vehicles for synthesis of other materials and devices.

The use of stabilizing agents for metal nanoparticles is not only important to avoid the particle aggregation but also in the size and shape control of these materials [8, 9]. Quaternary ammonium salts and thiols are used as nanoparticle stabilizing agents since they may provide both

**Electronic supplementary material** The online version of this article (doi:10.1007/s10971-012-2696-8) contains supplementary material, which is available to authorized users.

M. R. Nunes · J. Dupont · T. M. H. Costa · E. V. Benvenutti (✉)
Instituto de Química, UFRGS, Caixa Postal 15003, Porto Alegre, RS CEP 91501-970, Brazil
e-mail: benvenutti@iq.ufrgs.br

Y. Gushikem
Instituto de Química, UNICAMP, Caixa Postal 6154, Campinas, SP CEP 13083-970, Brazil

R. Landers
Instituto de Física Gleb Wataghin, UNICAMP, Caixa Postal 6165, Campinas, SP CEP 13083-970, Brazil

steric and electronic protection to the nanoparticles [10, 11]. In particular, ionic liquids are very versatile stabilizing and template agents for the generation of several nanomaterials [12–15]. It is also possible to use organosilanes containing amine, thiol or imidazolium groups as nanoparticle stabilizer in solid matrices [15–19]. These organosilanes can be used as molecular precursors to prepare new silica based hybrid materials that may combine both organic and inorganic properties.

A particular kind of organosilane precursors are the charged ones, which can be used to prepare ionic hybrid materials. Although the charged silsesquioxanes have been studied by few research groups, they present several important characteristics like water solubility, which enable to form films over metal or oxide surfaces allowing the application in different systems [20–23]. These charged silsesquioxanes were used as molecular precursors in sol–gel and grafting reactions to generate materials: with uniform porosity [24], with anisotropic organization imposed by the charged organic moiety [25], adsorbent for anionic dyes [26, 27], adsorbent for metal complex [28], long chain surfactants for dispersion of multiwall carbon nanotubes in ceramic matrices [29] and also materials for electrochemical sensors [26, 30]. The sol–gel method is very important to prepare silica based hybrid materials due to the slow reactivity of the silicon in sol–gel precursors that allows design the morphological and textural characteristics of the final material. Additionally the sol–gel products can be obtained in the form of powders, monoliths and films, enlarging the possibilities of applications [31, 32]. Thus, these materials show potential to stabilize metal nanoparticles by the sol–gel method, resulting in innovative materials. However, in general charged hybrids were few used as metal nanoparticle stabilizer [7, 15, 33].

In this work the charged silsesquioxane containing the charged 1,4-diazoniabicyclo[2.2.2]octane chloride group bonded in a bridged way (Fig. 1), was used as stabilizing agent of gold nanoparticles in liquid and powder form. The liquid dispersion was applied to prepare new material with catalytic activity, by using the sol–gel method.

## 2 Experimental section

The colloidal gold nanoparticle dispersions were prepared by reduction of chloriauric acid ($HAuCl_4$) by sodium borohydride ($NaBH_4$) in a water solution of silsesquioxane containing the charged 1,4-diazoniabicyclo[2.2.2]octane chloride group bonded in a bridged way (Fig. 1), assigned as dabcosil. The dabcosil silsesquioxane was prepared according to published procedure [25]. It was used 0.5 mL of 5 $10^{-3}$ mol $L^{-1}$ $HAuCl_4$ solution, which was added to 20 mL of dabcosil solution (8 g $L^{-1}$). In this solution it was added 10 mL of $NaBH_4$ 0.02 mol $L^{-1}$, resulting in a dark red solution assigned as Au-dispersion. The analysis by ultraviolet and visible spectroscopy (UV–Vis) of colloids containing gold nanoparticles were carried out in a Shimadzu UV 1601PC and collected in the range from 300 to 700 nm. The Au-dispersion was evaporated to form the solid assigned as Au-dabcosil. This solid was completely redispersed in water to form Au-redispersion. A part of the Au-dabcosil sample was storage and redispersed after 3 months, to result in Au-redispersion-3-months.

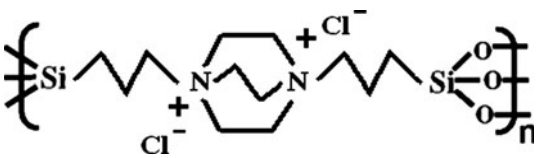


**Fig. 1** Structure of the water soluble silsesquioxane, containing the charged 1,4-diazoniabicyclo[2.2.2]octane chloride group

Transmission Electron Microscopy images of dispersions and of the solid were performed in JEOL JEM1200 microscope operating at 120 kV. The samples were dispersed in acetone with the aid of ultrasound bath and deposited on a copper grid coated with carbon. The nanoparticle diameter distribution was obtained by the Quantikov software, using several images.

Solid state NMR spectroscopy was performed on a Bruker 300/P spectrometer using the MAS (Magic angle) with CP (Cross-polarization) for solid Au-dabcosil and dabcosil (pure charged silsesquioxane). The $^{13}C$ experiments were obtained using pulse length of 1 ms and recycle delay of 2 s while the $^{29}Si$ measurements were made utilizing pulse length of 2.5 ms and recycle delay of 1 s. X-ray photoelectron spectra (XPS) were also obtained for solid Au-dabcosil and dabcosil samples using a hemispheric Specs VSW HA 100 spectrometer. X-ray diffraction patterns of the Au-dabcosil and dabcosil powdered samples were obtained with a Siemens diffractometer model D500 using CuK$\alpha$ as radiation source.

To apply the Au-dabcosil system as source of gold nanoparticles in the synthesis of new materials, a silica based hybrid xerogel was prepared. In this procedure, 2 mL of Au-dispersion were gelified in presence of 1 mL to tetraethylorthosilicate, using ethylic alcohol as solvent and HF as catalyst. The xerogel was characterized by $N_2$ adsorption–desorption isotherms using Micromeritics 3020 Krypton II equipment. The catalytic activity of xerogel was tested in the reduction of *p*-nitrophenol, which was conducted in a standard quartz cell with path length of 1 cm and 3 mL of volume. The solution of *p*-nitrophenol at concentration of 0.015 g $L^{-1}$ was adjusted at pH 10. This solution was first mixed with $NaBH_4$ 0.6 mol $L^{-1}$ aqueous solution, and after 10 mg of the xerogel catalyst was added and the absorption spectra were recorded by UV–Vis in a Shimadzu UV 1601PC.

## 3 Results and discussion

The Au-dispersion obtained is very stable for several months, and exhibits a typical UV–Vis spectrum, showing an absorption maximum at 527 nm (Fig. 2), typical of nanoparticles with diameter lower than 20 nm [34]. The Au-dispersion can be evaporated to form the solid assigned as Au-dabcosil, which is showed in the supplementary Fig. 1. This solid can be completely redispersed in water to form Au-redispersion, which displays the same UV–Vis spectrum of the Au-dispersion. The solid Au-dabcosil is very stable, since it can be redispersed after 3 months, to result in Au-redispersion-3-months that presents similar UV spectrum (Fig. 2).

The resulting solid Au-dabcosil, obtained from the Au-dispersion evaporation was analyzed by $^{13}C$ and $^{29}Si$ NMR, and the results are presented in Fig. 3a and b, respectively. The $^{13}C$ NMR spectrum of Au-dabcosil is practically the same obtained for pure charged dabcosil silsesquioxane, indicating that its structure did not undergo changes during the nanoparticle synthesis and drying process [25]. It can be observed that the relative intensity of $^{13}C$ due to carbon atom of hydrolysable methoxy group decreases its intensity in the Au-dabcosil sample (Fig. 3a), suggesting that this sample is more hydrolyzed and possibly more crosslinked

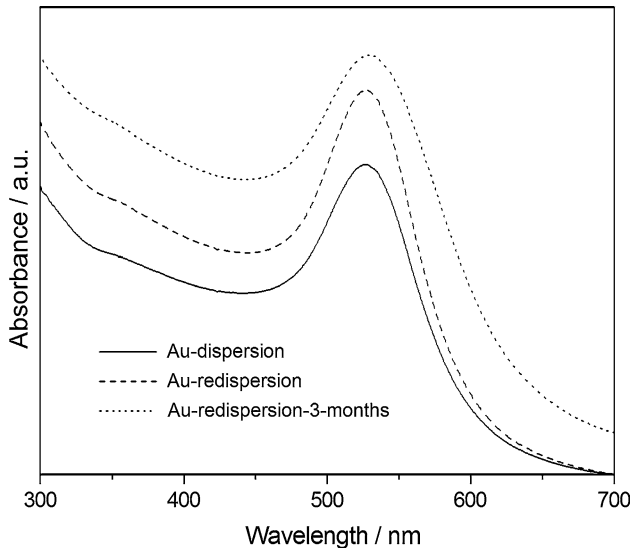


**Fig. 2** UV–Vis spectra of Au-dispersion, Au-redispersion and Au-redispersion-3-months

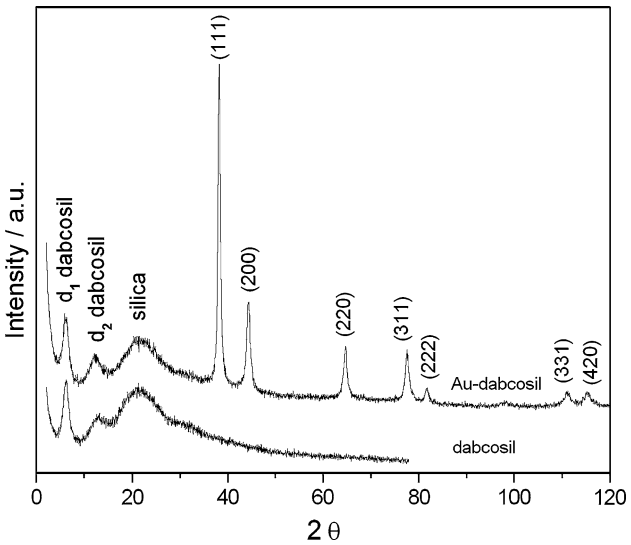


**Fig. 4** X-ray diffraction pattern of the dabcosil and Au-dabcosil

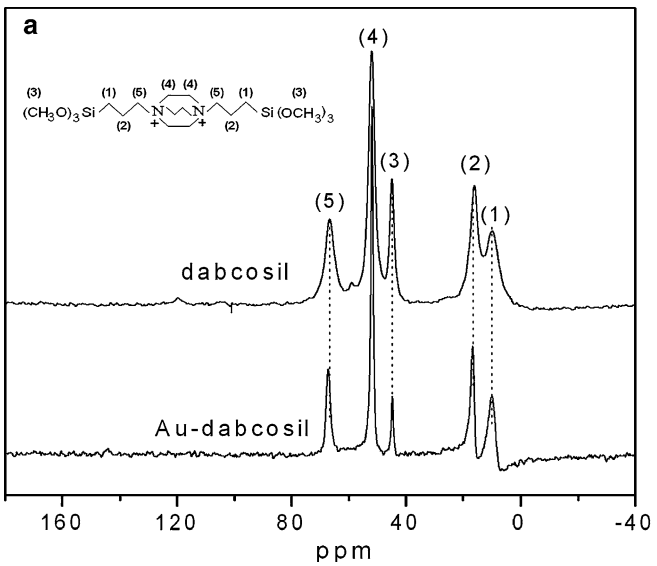


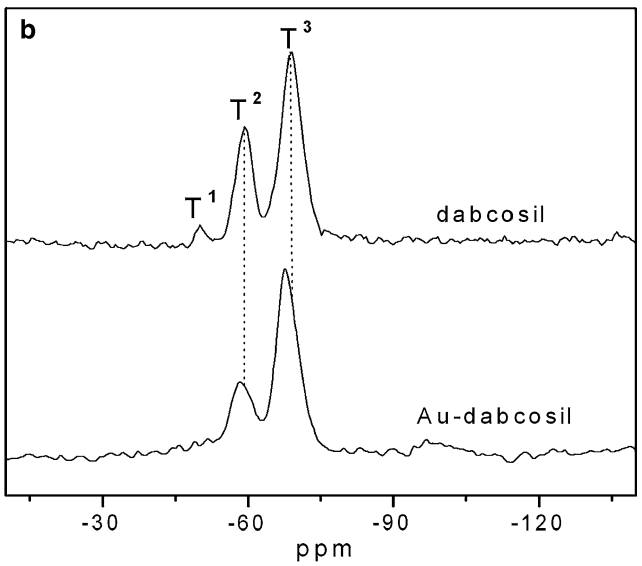


**Fig. 3** NMR spectra of dabcosil and Au-dabcosil. **a** $^{13}C$ and **b** $^{29}Si$

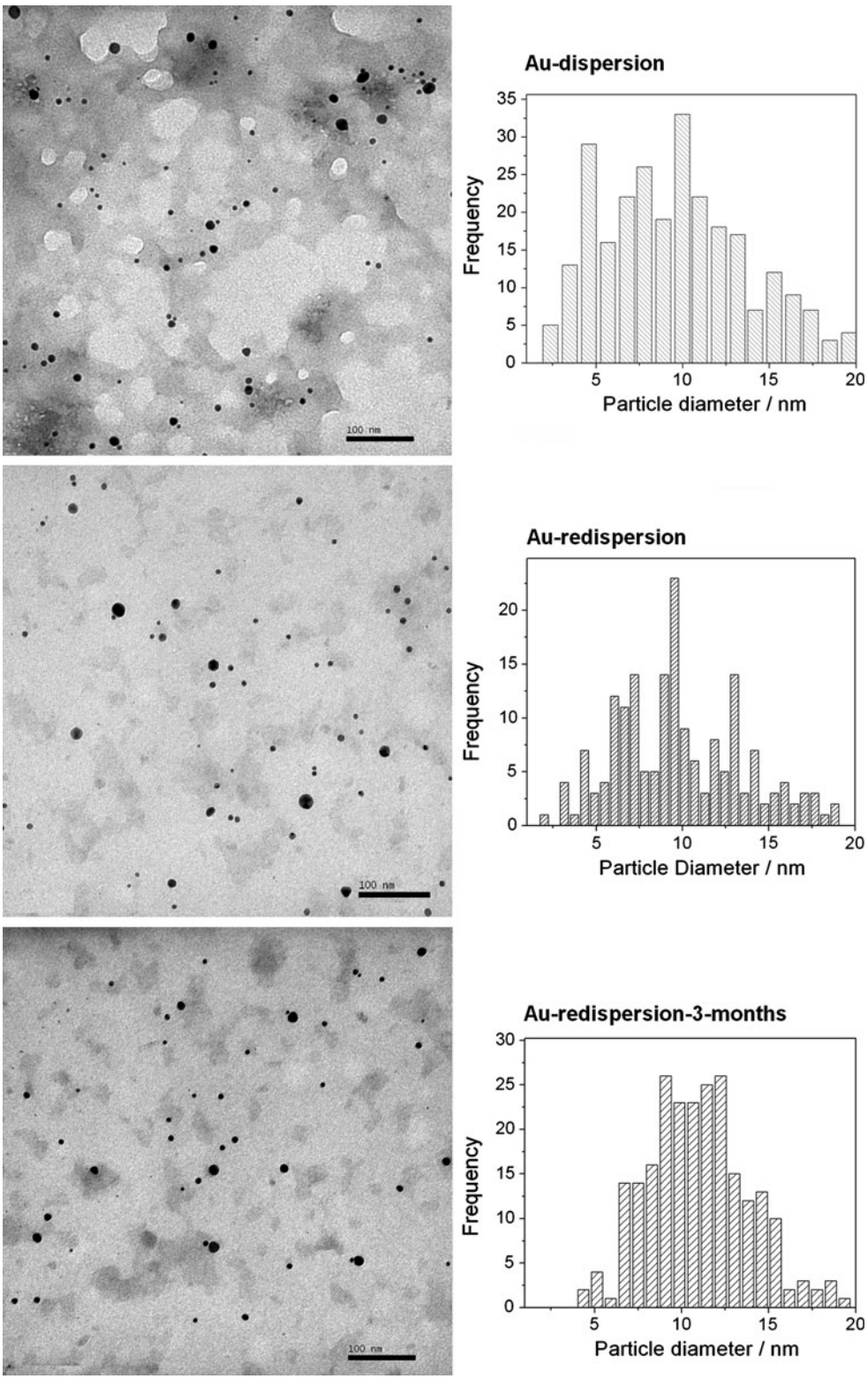


**Fig. 5** TEM images and particle size distribution of Au-dispersion, Au-redispersion and Au-redispersion-3-months

than pure dabcosil charged silsesquioxane. This hypothesis is also supported by the $^{29}$Si NMR results, presented in Fig. 3b. The $^{29}$Si spectrum of dabcosil silsesquioxane shows three peaks, characteristic of $T^1$ C–Si*$(OR)_2(OSi)$, $T^2$ C–Si*$(OR)(OSi)_2$ and $T^3$ C–Si $(OSi)_3$ species at −50.0, −59.3 and −69.0 ppm, respectively [25], while the Au-dabcosil sample shows only the $T^2$ and $T^3$ species, at −58.3 and −67.8 ppm, respectively.

The Au-dabcosil and pure dabcosil silsesquioxane were characterized by X-ray diffraction (Fig. 4). In the angle region $2\theta$ below 30°, it was observed a large peak for both samples, with angle $2\theta$ near 22°, which is characteristic of silica, and the peaks at 6.2° and 12.5°, which correspond to the interplanar distances of 1.43 and 0.71 nm. These two peaks indicate the existence of organized structure imposed by the presence of the charged organic group, as already reported [25]. This organization was not disturbed by the presence of gold nanoparticles. For the Au-dabcosil sample, diffraction peaks were clearly observed in the high angle region, $2\theta$ above 30°. These peaks correspond to the gold close packed cubic structure according to Joint Committee on Powder Diffraction Standards (JCPDS) card 65-2870. The calculated mean diameter of 14.7 nm for the Au(0) nanoparticles, using the Scherrer equation, is in good agreement to that found by TEM, as discussed in sequence.

Typical TEM images of Au-dispersion, Au-redispersion and Au-redispersion-3-months are presented in Fig. 5, simultaneously with the particle size distribution diagrams. The average gold nanoparticle sizes for Au-dispersion, Au-redispersion and Au-redispersion-3-months were, respectively, 9.3, 9.3 and 10.6 nm, with standard deviation lower than 4.0 nm for the three dispersions. These results are in agreement to the UV–Vis spectra confirming that the average gold nanoparticle size is smaller than 20 nm and remains the same after the redispersion.

**Table 1** XPS analysis

| Sample | Binding energies/eV | | | | | |
|---|---|---|---|---|---|---|
| | $Au^0$ $4f_{7/2}$ | $Au^0$ $4f_{5/2}$ | $Au^+$ $4f_{7/2}$ | $Au^+$ $4f_{5/2}$ | Cl $2p_{3/2}$ | Cl $2p_{1/2}$ |
| Dabcosil | | | | | 196.8 | 198.4 |
| Au-dabcosil | 83.9 | 87.6 | 85.2 | 88.7 | 197.6 | 199.2 |

Binding energy values for 4f gold and 2p chlorine peaks, obtained from XPS spectrum of solid Au-dabcosil, are showed in the Table 1. It was observed the presence of metallic gold in major proportion in a relation about 3/1 of $A^0/Au^+$ [35, 36]. Regarding the chlorine binding energies, it was detected inorganic chloride for dabcosil and Au-dabcosil. However there is an increasing of 0.8 eV in the Cl $2p_{1/2}$ for sample containing gold nanoparticles, suggesting an interaction between chloride ions and gold nanoparticles, contributing to their stabilization [10].

To explore the stability and possibility of application of this new system, the Au-dispersion was applied as gold nanoparticle vehicle in the synthesis of silica based hybrid material using the sol–gel method. In this method, the precursor components, such as tetraethylorthosilicate, charged silsesquioxane and nanoparticles are dispersed in a nanometric level in an initial liquid, which in sequence undergo polycondensation reactions forming homogeneous

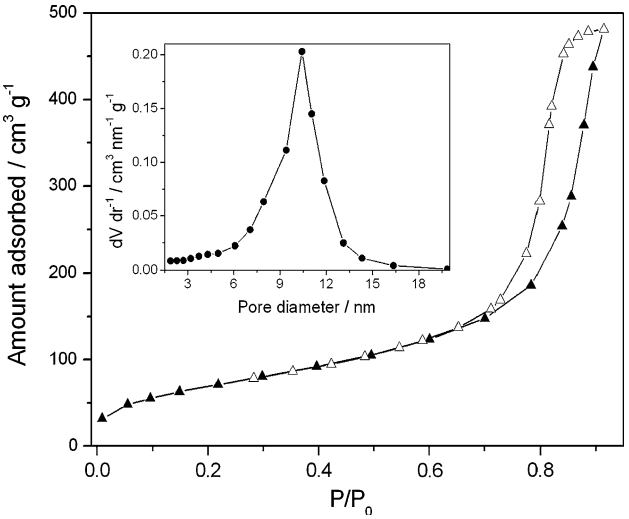


**Fig. 7** $N_2$ adsorption–desorption isotherms of xerogel. *Inset* figure: BJH pore size distribution

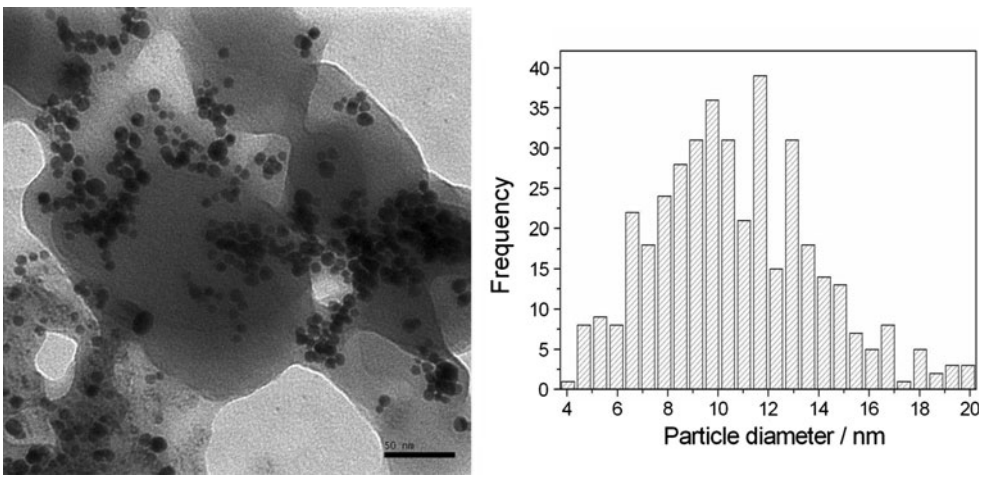


**Fig. 6** TEM image and particle size distribution of gold nanoparticles dispersed in hybrid xerogel

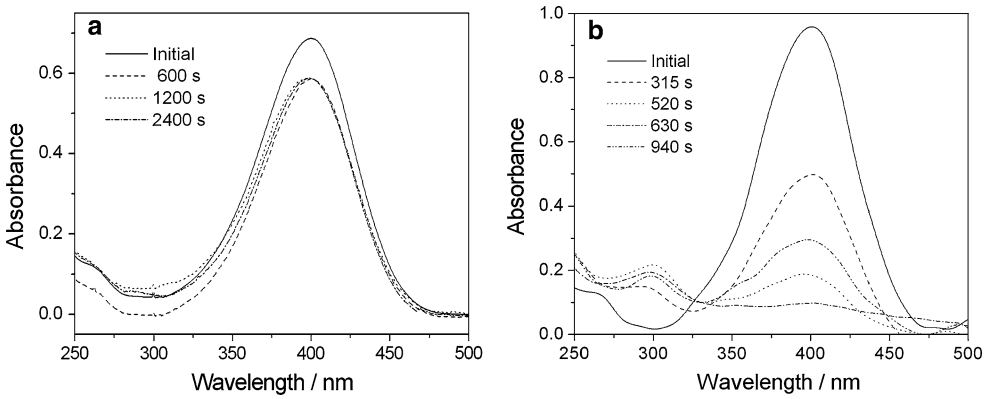


**Fig. 8** UV–Vis spectra of reaction in solution of *p*-nitrophenol reduction to *p*-aminophenol at different times. **a** in the absence of catalyst; **b** in the presence of xerogel catalyst

and amorphous solid, maintaining the high dispersion of the components. Thus the gold nanoparticles become dispersed in all sample, bulk and surface. The resulting xerogel is transparent and presents reddish colour typical of gold nanoparticles, and a picture is showed in the supplementary Fig. 2. TEM image of the xerogel is presented in Fig. 6, simultaneously with the particle size distribution diagram. It can be observed a higher nanoparticle concentration than in the liquid dispersions; however the average size of gold nanoparticles remains the same, 10.5 nm with a standard deviation of 4 nm, indicating that the coalescence of the nanoparticles did not occur.

The $N_2$ adsorption–desorption isotherms of the xerogel are showed in the Fig. 7, together with the BJH pore size distribution curves. It was observed a type IV isotherm, typical of mesoporous materials [32, 37], with predominant pore diameter near 10 nm, characteristic of amorphous xerogels obtained in the presence of HF [32]. From the BET multipoint method, it was obtained a specific surface area of $260 \pm 15$ $m^2g^{-1}$, making this system very promising as heterogeneous catalyst. Therefore, the catalytic properties of the xerogel were studied and the evolution of the reaction of *p*-nitrophenol being reduced by sodium borohydride, in the absence and presence of catalyst, is showed in the Fig. 8. The reduction process of *p*-nitrophenol using sodium borohydride is monitored by measuring the UV–Vis spectra at different time t. The characteristic peak at 400 nm ascribed to *p*-nitrophenol decreases gradually with time, while a new peak at 310 nm indicates the appearance of a new reduced product, *p*-aminophenol. This reaction catalyzed by gold nanoparticle was reported for the first time in 2001 [38] and it has been widely applied as model reaction to evaluate the catalytic rate of new catalyst systems containing gold nanoparticles. Different matrices have been used as support for immobilization of gold nanoparticles as polymer, resins [39–42], carbon nanotube [43], natural matrices [44] and inorganic matrices such alumina, silica and clay [45–49]. For these materials the kinetic constant of the reaction are in a range from $3.3\ 10^{-5}$ to $3.6\ 10^{-2}$ $s^{-1}$. In the present work the reduction reaction of *p*-nitrophenol using the hybrid xerogel was performed at 298 K, and the kinetic constant of the reaction was determined as $3.5\ 10^{-3}$ $s^{-1}$. The value found was in the same range of the previous reports. However, it is important to point out that in the present work the amount of gold was very low. Considering the weight of catalyst used, the amount of gold did not exceed $8.3\ 10^{-9}$ mol of gold atoms in the form of nanoparticles, making this system promising.

## 4 Conclusions

The charged water soluble dabcosil silsesquioxane, containing the charged 1,4-diazoniabicyclo[2.2.2]octane group was successfully applied as stabilizer for gold nanoparticle synthesis, without addition of other components. The gold nanoparticles were smaller than 15 nm. The organic moiety of silsesquioxane does not undergo structural changes in the presence of gold nanoparticles. The gold nanoparticles dispersion can be evaporated, transformed in solid form, stored by several months and completely redispersed in water, without any changes in the optical and morphological properties. Therefore, this system opens the possibility to easy storage and transport of metal nanoparticles in solid form and allows reusing them as vehicle of gold nanoparticles in the preparation of new materials with catalytic activity.

**Acknowledgments** We thank to Conselho Nacional de Desenvolvimento Científico e Tecnológico, Fundação de Amparo à Pesquisa do Estado do Rio Grande do Sul and Coordenação de Aperfeiçoamento Pessoal de Nível Superior for grants and financial support. We also thank the Centro de Microscopia Eletrônica da Universidade Federal do Rio Grande do Sul for TEM images.

## References

1. Jin Y, Li A, Hazelton SG, Liang S, John CL, Selid PD (2009) Amorphous silica nanohybrids: synthesis, properties and applications. Coord Chem Rev 253:2998–3014

2. Vidotti M, Carvalhal RF, Mendes RK, Ferreira DCM, Kubota LT (2011) Biosensors based on gold nanostructures. J Braz Chem Soc 22:3–20
3. Pingarrón JM, Paloma Yáñez-Sedeño P, González-Cortés A (2008) Gold nanoparticle-based electrochemical biosensors. Electrochim Acta 53:5848–5866
4. Zhang X, Guo Q, Cui D (2009) Recent advances in nanotechnology applied to biosensors. Sensors 9:1033–1053
5. Gabaldon JP, Bore M, Datye AK (2007) Mesoporous silica supports for improved thermal stability in supported Au catalysts. Top Catal 44:253–262
6. Laranjo MT, Kist KBL, Benvenutti EV, Gallas MR, Costa TMH (2011) Gold nanoparticles enclosed in silica xerogels by high-pressure processing. J Nanopart Res 13:4987–4995
7. Jin Y, Wang P, Yin D, Liu J, Qiu H, Yu N (2008) Gold nanoparticles stabilized in a novel periodic mesoporous organosilica SBA-15 styrene epoxidation. Micropor Mesopor Mater 111: 569–576
8. Bonnemann H, Richards RM (2001) Nanoscopic metal particles—synthetic methods and potential applications. Eur J Inorg Chem 10:2455–2480
9. Peterle T, Ringler P, Mayor M (2009) Gold nanoparticles stabilized by acetylene-functionalized multidentate thioether ligands: building blocks for nanoparticle superstructures. Adv Funct Mater 19:3497–3506
10. Ott LS, Finke RG (2007) Transition-metal nanocluster stabilization for catalysis: a critical review of ranking methods and putative stabilizers. Coord Chem Rev 251:1075–1100
11. Peterle T, Ringler P, Mayor M (2009) Gold nanoparticles stabilized by acetylene-functionalized multidentate thioether ligands: building blocks for nanoparticle superstructures. Adv Funct Mater 19:3497–3506
12. Safavi A, Zeinali S (2010) Synthesis of highly stable gold nanoparticles using conventional and geminal ionic liquids. Coll Surf A 362:121–126
13. Dupont J, de Souza RF, Suarez PAZ (2002) Ionic liquid (molten salt) phase organometallic catalysis. Chem Rev 102:3667–3692
14. Khatri OP, Adachi K, Murase K, Okazaki K, Torimoto T, Tanaka N, Kuwabata S, Sugimura H (2008) Self-assembly of ionic liquid (bmi-pf6)-stabilized gold nanoparticles on a silicon surface: chemical and structural aspects. Langmuir 24:7785–7792
15. Ma Z, Yu J, Dai S (2010) Preparation of inorganic materials using ionic liquids. Adv Mater 22:261–285
16. Chang C–C, Chen P-H, Chang C-M (2008) Preparation and characterization of acrylic polymer–nanogold nanocomposites from 3-mercaptopropyltrimethoxysilane encapsulated gold nanoparticles. J Sol-Gel Sci Technol 47:268–273
17. Bharathi S, Lev O (1997) Direct synthesis of gold nanodispersions in sol-gel derived silicate sols, gels and films. Chem Commun 23:2303–2304
18. Flavel BS, Nussio MR, Quinton JS, Shapter JG (2009) Adhesion of chemically and electrostatically bound gold nanoparticles to a self-assembled silane monolayer investigated by atomic force volume spectroscopy. J Nanopart Res 11:2013–2022
19. Shibata S, Miyajima K, Kimura Y, Yano T (2004) Heat-induced precipitation and light-induced dissolution of metal (Ag & Au) nanoparticles in hybrid film. J Sol-Gel Sci Technol 31:123–130
20. Arenas LT, Langaro A, Gushikem Y, Moro CC, Benvenutti EV, Costa TMH (2003) 3-*n*-Propyl-1-azonia-4-azabicyclo[2.2.2] octanechloride silsesquioxane: a new water soluble polymer. J Sol-Gel Sci Technol 28:51–56
21. da Trindade CM, Stoll GC, Pereira AS, Costa TMH, Benvenutti EV (2009) An innovative series of layered nanostructured aminoalkylsilica hybrid material. J Braz Chem Soc 20:737–743
22. Gushikem Y, Benvenutti EV, Kholin YV (2008) Synthesis and applications of functionalized silsesquioxanes polymers attached to organic and inorganic matrices. Pure Appl Chem 80: 1593–1611
23. Pereira MB, Michels AF, Gay DSF, Benvenutti EV, Costa TMH, Horowitz F (2010) Silica-based hybrid films with double-charged diazoniabicyclo[2.2.2]octane chloride group: preparation and optical properties related to transition layer structure. Opt Mater 32:1170–1176
24. Arenas LT, Dias SLP, Moro CC, Costa TMH, Benvenutti EV, Lucho AMS, Gushikem Y (2006) Structure and property studies of hybrid xerogels containing bridged positively charged 1,4-diazoniabicycle[2.2.2] octane dichloride. J Coll Interf Sci 297: 244–250
25. Arenas LT, Pinheiro AC, Ferreira JD, Livotto PR, Pereira VP, Gallas MR, Gushikem Y, Costa TMH, Benvenutti EV (2008) Anisotropic self-organization of hybrid silica based xerogels containing bridged positively charged 1,4-diazoniabicycle[2.2.2]octane chloride group. J Coll Interf Sci 318:96–102
26. Arenas LT, Gay DSF, Moro CC, Dias SLP, Azambuja DS, Gushikem Y, Costa TMH, Benvenutti EV (2008) Brilliant yellow dye immobilized on silica and silica/titania based hybrid xerogels containing bridged positively charged 1,4-diazoniabicycle[2.2.2]octane: preparation, characterization and electrochemical properties study. Micropor Mesopor Mater 112: 273–283
27. Gay DSF, Fernandes THM, Amavisca CV, Cardoso NF, Benvenutti EV, Costa TMH, Lima EC (2010) Silica grafted with a silsesquioxane containing the positively charged 1,4-diazoniabicyclo[2.2.2]octane group used as adsorbent for anionic dye removal. Desalination 258:128–135
28. Splendore G, Benvenutti EV, Kholin YV (2005) Cellulose acetate-$Al_2O_3$ hybrid material coated with n-propyl-1,4-diazabicyclo[2.2.2]octane chloride. Preparation, characterization and study of some metal halides adsorption from ethanol solution. J Braz Chem Soc 16:147–152
29. Silva PR, Almeida VO, Machado GB, Benvenutti EV, Costa TMH, Gallas MR (2012) A surfactant-based dispersant for multiwall carbon nanotubes to prepare ceramic composites by a sol-gel method. Langmuir 28:1447–1452
30. de Jesus CG, dos Santos V, Canestraro CD, Zucoloto V, Fujiwara ST, Gushikem Y, Wohnrath K, Pessoa CA (2011) Silsesquioxane as a new building block material for modified electrodes fabrication and application as neurotransmitters sensors. J Nanosci Nanotechnol 11:3499–3508
31. Sanchez C, Rozes L, Ribot F, Laberty-Robert C, Grosso D, Sassoye C, Boissiere C, Nicole L (2010) 'Chimie douce'': a land of opportunities for the designed construction of functional inorganic and hybrid organic-inorganic nanomaterials. C R Chimie 13:3–39
32. Benvenutti EV, Moro CC, Costa TMH, Gallas MR (2009) Silica based hybrid materials obtained by the sol-gel method. Quim Nova 32:1926–1933
33. Shin JY, Lee BS, Jung Y, Kim SJ, Lee S (2007) Palladium nanoparticles captured onto spherical silica particles using a urea cross-linked imidazolium molecular band. Chem Comm 2007: 5238–5240
34. Yguerabide J, Yguerabide EE (1998) Light-scattering submicroscopic particles as highly fluorescent analogs and their use as tracer labels in clinical and biological applications. Anal Biochem 262:137–156
35. Delannoy L, Fajerwerg K, Lakshmanan P, Potvin C, Méthivier C, Louis C (2010) Supported gold catalysts for the decomposition of VOC: total oxidation of propene in low concentration as model reaction. Appl Catal B 94:117–124
36. Ma S, Li G, Wang X (2010) Direct synthesis of hydrogen peroxide from $H_2/O_2$ and oxidation of thiophene over supported gold catalysts. Chem Eng J 156:532–539

37. Gregg SJ, Sing KSW (1982) Adsorption, surface area and porosity, Chap 3, 2nd edn. Academic Press, London
38. Pradhan N, Pal A, Pal T (2001) Catalytic reduction of aromatic nitro compounds by coinage metal nanoparticles. Langmuir 17: 1800–1802
39. Praharaj S, Nath S, Ghosh SK, Kundu S, Pal T (2004) Immobilization and recovery of Au nanoparticles from anion exchange resin: resin-bound nanoparticle matrix as a catalyst for the reduction of 4-nitrophenol. Langmuir 20:9889–9892
40. Panigrahi S, Basu S, Praharaj S, Pande S, Jana S, Pal A, Ghosh SK, Pal T (2007) Synthesis and size-selective catalysis by supported gold nanoparticles: study on heterogeneous and homogeneous catalytic process. J Phys Chem C 111:4596–4605
41. Chen X, Zhao D, An Y, Zhang Y, Cheng J, Wang B, Shi L (2008) Formation and catalytic activity of spherical composites with surfaces coated with gold nanoparticles. J Coll Interf Sci 322: 414–420
42. Kuroda K, Ishida T, Haruta M (2009) Reduction of 4-nitrophenol to 4-aminophenol over Au nanoparticles deposited on PMMA. J Mol Catal A 298:7–11
43. Tang J, Tang D, Su B, Huang J, Qiu B, Chen G (2011) Enzyme free electrochemical immunoassay with catalytic reduction of p-nitrophenol and recycling of p-aminophenol using gold nanoparticles-coated carbon nanotubes as nanocatalysts. Biosens Bioelectron 26:3219–3226
44. Sharma NC, Sahi SV, Nath S, Parsons JG, Torresdey JLG, Pal T (2007) Synthesis of plant-mediated gold nanoparticles and catalytic role of biomatrix-embedded nanomaterials. Environ Sci Technol 41:5137–5142
45. Lee KY, Lee YW, Kwon K, Heo J, Kim J, Han SW (2008) One-step fabrication of gold nanoparticles-silica composites with enhanced catalytic activity. Chem Phys Lett 453:77–81
46. Dinda E, Rashid MH, Biswas M, Mandal TK (2010) Redox-active ionic-liquid-assisted one-step general method for preparing gold nanoparticle thin films: applications in refractive index sensing and catalysis. Langmuir 26:17568–17580
47. Jana D, Dandapat A, De G (2010) Anisotropic gold nanoparticle doped mesoporous boehmite films and their use as reusable catalysts in electron transfer reactions. Langmuir 26:12177–12184
48. Koga H, Kitaoka T (2011) One-step synthesis of gold nanocatalysts on a microstructured paper matrix for the reduction of 4-nitrophenol. Chem Eng J 168:420–425
49. Hallett-Tapley GL, Charles-Oneil L, Crites C-OL, González-Béjar M, McGilvray KL, Netto-Ferreira JC, Scaiano JC (2011) Dry photochemical synthesis of hydrotalcite, $\gamma$-Al2O3 and $TiO_2$ supported gold nanoparticle catalysts. J Photochem Photobiol A 224:8–15